J. Membrane Biol. 70, 199–216 (1982)

The Journal of
Membrane Biology

The Kinetics of Intramolecular Cross-Linking of the Band 3 Protein in the Red Blood Cell Membrane by 4,4′-Diisothiocyano Dihydrostilbene-2,2′-Disulfonic Acid (H_2DIDS)

L. Kampmann, S. Lepke, H. Fasold*, G. Fritzsch, H. Passow
Max-Planck-Institut für Biophysik, Frankfurt am Main, Germany

Summary. The two isothiocyanate groups of the anion transport inhibitor 4,4′-diisothiocyano dihydrostilbene-2,2′-disulfonate (H_2DIDS) may react covalently with two lysine residues called *a* and *b* that reside on the chymotryptic 60,000 Dalton and 35,000 Dalton segments, respectively, of the band 3 protein of the human erythrocyte membrane. Under suitable conditions, the reaction leads to the establishment of intramolecular cross-links between *a* and *b* (M.L. Jennings & H. Passow, 1979, *Biochim. Biophys. Acta* **554**:498–519). In the present work, the time course of the reactions with *a* and *b*, and of the establishment of the cross-link were investigated experimentally and compared with simple mathematical models of the reaction sequence. The rates of reaction with *a* and *b* were found to increase with increasing pH. Regardless of pH, the rate of reaction with *a* exceeds that with *b* several-fold. Once the H_2DIDS molecule has reacted with *a*, the rate of the subsequent reaction of the other isothiocyanate group with *b* is reduced by about 1/30. The reactions that follow the unilateral attachment to site *b* are not yet clear. A more detailed analysis of the time course of the cross-linking reaction suggests that a satisfactory description of the kinetics requires the assumption that the H_2DIDS binding site may exist in two different states, and that the transition from one state to the other is associated with changes of the reactivities of either lys *a* alone or of both lys *a* and *b*. This led to the formulation of the two-states model of the H_2DIDS binding site, which is supported by other pieces of independent evidence. The analysis of the pH dependence of the rate of thiocyanylation of *b* shows that the apparent pK value of that lysine residue is about 9.9 to 10.0 and hence slightly lower than the intrinsic pK of a lysine residue in an aqueous environment.

Key words red cell membrane · band 3 protein · anion transport · H_2DIDS · 4,4′-diisothiocyano dihydrostilbene-2,2′-disulfonic acid · cross-linking

Abbreviations

APMB = 2-(4-amino-3-sulfophenyl)-6-methyl-7-benzothiazolsulfonic acid
DANS-Cl = 5-(dimethylamino)naphthalenesulfonyl chloride
DAS = diacetamido stilbene-2,2′-disulfonate
DBDS = 4,4′-dibenzoyl stilbene-2,2′-disulfonate
DNDS = 4,4′-dinitro stilbene-2,2′-disulfonate
EDTA = ethylenediaminetetraacetic acid
H_2DIDS = 4,4′-diisothiocyano dihydrostilbene-2,2′-disulfonic acid
N_2ph-F = 1-fluoro-2,4-dinitrobenzene
PCMBS = *para*-chloromercuribenzoate
SDS = sodium dodecyl sulfate

* *Present address:* Biochemisches Institut der Johann-Wolfgang-Goethe-Universität, Frankfurt am Main, Germany

Introduction

An isothiocyanate derivative of a stilbene disulfonic acid was first applied to the study of biological membranes by Maddy in 1964. The discovery that such derivatives inhibit anion transport in red cells (Knauf & Rothstein, 1971) and react nearly exclusively with the band 3 protein in the red cell membrane (Cabantchik & Rothstein, 1974; Passow et al., 1975) established their usefulness for the study of the molecular mechanism of anion transport.

At complete inhibition of anion transport, about 1×10^6 molecules per red cell are bound to the band 3 region of SDS polyacrylamide gel electropherograms of the red cell membrane (Passow et al., 1975; Zaki, Fasold, Schuhmann & Passow, 1975; Halestrap, 1976; Lepke, Fasold, Pring & Passow, 1976; Ship, Shami, Breuer & Rothstein, 1977; and others). This corresponds roughly to the only existing estimate of the number of band 3 molecules in the red cell membrane (Steck, 1978) and suggests a 1:1 stoichiometry of inhibition.

The binding of the most widely used diisothiocyanate derivative, H_2DIDS, takes place in two steps: The first is reversible and is complete within less than one second. The second leads to the slow establishment of covalent bonds via the NCS groups of the inhibitor. Under suitable conditions, this latter process results in the formation of intramolecular cross-links between two adjacent amino groups that reside on two different segments of the peptide chain of the band 3 molecule (Jennings

0022-2631/82/0070-0199 $03.60

& Passow, 1979). Intermolecular cross-linking has not yet been observed.

The molecular properties on which the reversible binding of the inhibitors depend have been studied in much detail. Similar to many other inhibitors of anion transport (Cousin & Motais, 1978) the behavior of the noncovalently binding analogues of H_2DIDS is largely determined by their hydrophobicity and by their capacity to accept electrons from suitable donors on the band 3 molecule (as defined by the so-called Hammett constant) (Barzilay, Ship & Cabantchik, 1979). In addition, the presence of the two negative charges of the sulfonic acid seems to play a role. Binding of H_2DIDS and of certain of its analogues does not alter the electrophoretic mobility of the red cell as a whole (G.F. Fuhrmann & H. Passow, *unpublished*) and leads to the reduction of the signal of a spin labeled analogue of H_2DIDS (B. Lammel, K.F. Schnell, H. Fasold & H. Passow, *unpublished*). This indicates that the amphiphilic molecule becomes at least partly buried and immobilized upon reversible binding.

The affinity of H_2DIDS to combine reversibly with the band 3 molecule is quite high as indicated by an apparent K_I value of about 0.1 μM in Cl^- containing media (Shami, Rothstein, Knauf & McCulloch, 1978). Other purely noncovalently binding analogues (e.g., DNDS, DBDS) also have low apparent K_I values (Barzilay et al., 1979; Fröhlich, 1982). These K_I values depend on the Cl^- concentration in the medium, suggesting competition between the substrate and the inhibitor (Shami et al., 1978; Fröhlich, 1982). Nevertheless, in contrast to previous suggestions, it appears that the interactions between the binding of substrate and inhibitor do not necessarily reflect a competition for the substrate binding site ("transfer site") but possibly "allosteric competition" (Passow et al., 1980*a*) that is due to allosteric interactions between the substrate binding site and the H_2DIDS binding site (Passow, 1982).

H_2DIDS and its noncovalently binding analogues do not penetrate (Cabantchik & Rothstein, 1974) and inhibit anion transport only when applied to the outer membrane surface (Passow et al., 1975; Zaki et al., 1975; Kaplan, Scorah, Fasold & Passow, 1976; Cabantchik & Rothstein, 1974). This suggests that the H_2DIDS binding site is only exposed to the outer membrane surface, regardless of whether the transfer site is in contact with the inner or outer membrane surface. However, the conformation of the transport protein at the H_2DIDS binding site changes considerably when the transfer site is gradually saturated with substrate anions (Passow et al., 1980*b*; Passow, Fasold, Jennings & Lepke, 1982). Thus the allosteric interactions between the substrate binding sites and the H_2DIDS binding site are reflected not only by the inhibition of anion transport by H_2DIDS but also by the modification of the H_2DIDS binding site by substrate binding.

In view of the close relationship between transport and H_2DIDS binding, it seemed useful to supplement the existing information on reversible H_2DIDS binding by a study of the kinetics of covalent bond formation. For this purpose we have extended the previous work of Lepke et al. (1976) and of Ship et al. (1977) on the time course of covalent H_2DIDS binding by a more detailed study that takes into account that the H_2DIDS molecule has two NCS-groups that are capable of reacting with two lysine residues on different segments of the band 3 peptide, thereby establishing the intramolecular cross-link mentioned above.

To follow the cross-linking reaction we adapted the procedure of Jennings and Passow (1979). We exposed the red cell membrane to external chymotrypsin. This leads to the cleavage of the band 3 protein into two fragments of 60 K and 35 K, without interfering with anion transport or the inhibition of the transport by H_2DIDS or other agents. Apparently tertiary and quaternary forces preserve the original conformation of the transport protein even after the hydrolysis of the chymotrypsin-sensitive peptide bond. Subsequently, the red cells were exposed to an excess of H_2DIDS. This leads to a saturation of noncovalent binding to band 3 within a time that is negligibly small compared to the time required for covalent bond formation. Thereafter, covalent bond formation was followed by removing, in suitable time intervals, the unreacted and the reversibly bound H_2DIDS by washing with bovine serum albumin, isolating the membranes, and subjecting them to SDS gel electrophoresis. This allows one to separate the 35 K and 60 K fragments from one another and from the reconstituted 95 K band that is the result of formation of the cross-links between the two fragments. Using radioactively labeled H_2DIDS, it was possible to follow the time course of unilateral attachment to the 60 K and 35 K fragments as well as the time course of the cross-linking reaction. The kinetics measured by this method follows the most simple reaction scheme for a cross-linking reaction only approximately. The deviations can be explained on the assumption that the H_2DIDS binding site may exist in two different conformations in which one or both lysine residues assume different reactivities towards the isothiocyanate groups of the H_2DIDS molecule.

The rate of thiocyanylation of the two lysine

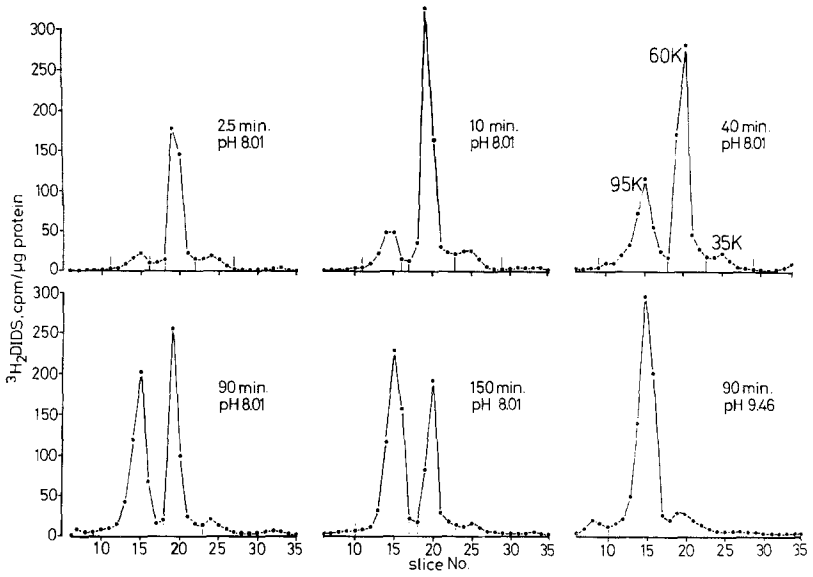

Fig. 1. Time course of labeling and cross-linking with $^3H_2$DIDS of the chymotryptic fragments of the band 3 protein. The three peaks on the SDS polyacrylamide gel electropherograms are located (from left to right) at 95 K, 60 K and 35 K. Labeling took place at 37 °C for the times indicated in the panels in the presence of a large excess of $^3H_2$DIDS in the medium. The last panel, designated *90 min, pH 9.46*, shows a control with cross-linking completed. Under these conditions, the electropherogram shows some labeling of spectrin and of other membrane proteins that should not be confused with the 35 K band

residues should depend on pH. We have, therefore, measured the kinetics of cross-linking at a range of pH values and have determined the apparent pK value that governs one of the various reaction steps. Since it is difficult to discriminate between effects of pH on the dissociation of the lysine residues that are directly involved in the thiocyanylation reaction and pH dependent conformational changes that affect the local reaction conditions allosterically, the interpretation of the derived pK value remains speculative.

Materials and Methods

Biochemical Methods

All experiments were performed with 0 Rh^+ blood from apparently healthy donors. After withdrawal the blood was stored at 4 °C in acid citrate dextrose for 2 to 5 days. Before use the cells were centrifuged down, the buffy coat was removed, and the sediment was washed three times with EDTA standard buffer, pH 7.4 (1 mM Na_2SO_4, 20 mM EDTA, 130 mM NaCl). The final sediment was resuspended to give a hematocrit of 10% and exposed to chymotrypsin (1 mg/ml suspension, 37 °C) for 1 hr. The treated cells were then washed twice with EDTA standard buffer, pH 7.4, containing 0.5% bovine serum albumin. Two further washes were carried out in the same buffer without albumin present. The pH of the buffer was adjusted to the values desired for the subsequent $^3H_2$DIDS treatment. To facilitate the hydrogen ion equilibration the cells were incubated between the washes at 37 °C for 5 min. If not explicitly stated otherwise, the $^3H_2$DIDS treatment was carried out at 37 °C, at a H_2DIDS concentration of 10 µM and a hematocrit of 10%. For sampling, the cross-linking reaction was stopped by rapidly diluting aliquots of the cell suspension with four times their volumes of ice cold buffer, pH 4.0, containing 0.5% bovine serum albumin and further washing at 0 °C in EDTA standard buffer, pH 7.0.

It should be recalled that treatment with chymotrypsin neither alters anion transport nor the stoichiometry of the reaction of band 3 with $^3H_2$DIDS. The concentration required for 50% inhibition (apparent $K_I = (2.89 \pm 0.17)$ µM, with or without chymotrypsin) by the noncovalently binding H_2DIDS analogue DNDS remains unchanged, and the establishment of the cross-links can be demonstrated regardless of whether the cells are first chymotrypsinized and then exposed to H_2DIDS, or *vice versa*. We preferred to chymotrypsinize prior to exposure to H_2DIDS. This enables one to time the termination of the cross-linking reaction more accurately than the alternative procedure, since it avoids the lengthy exposure to chymotrypsin after sampling. During this exposure, it is difficult to prevent the continuation of the cross-linking reaction of unilaterally bound H_2DIDS molecules, and hence the time of sampling remains less well determined than by the procedure described above.

The experiments represented in Fig. 4*a* were performed with resealed, hemoglobin-free red cell ghosts that had been prepared by hemolysis on an agarose column, according to Wood. For a description of the method and of the properties of the ghosts the reader is referred to a recent review (Wood & Passow, 1981).

Hemoglobin-free membranes were isolated by hemolyzing and washing in a medium containing 1% saponin, 10 mM KCl, 5 mM EDTA, pH 7.0, 0 °C. Peripheral membrane proteins were removed by "stripping" in 10 volumes of phosphate buffer (5 mM, pH 7.0) containing 10 mM PCMBS for 30 min at 0 °C. The cells were centrifuged for 20 min (Sorvall rotor SS 34, 20,000 rpm), and the pellet was washed once with ice-cold distilled water. For measuring the $^3H_2$DIDS binding and the protein concentration (method of Lowry; *see* Peterson, 1979), the membranes were dissolved in one volume of 5% SDS, heated at 100 °C for 3 min, and then diluted to a final concentration of 0.5% SDS. After addition of glycerol, dithiothreitol and bromophenol blue, polyacrylamide gel electrophoresis was performed as described previously (Zaki et al., 1975). Gels were run in duplicates, one was stained with Coomassie Brillant Blue G 250, the other was cut into 30–40 slices. For radioactivity counting, the slices were first digested in 1 ml Soluene (Packard) for 6 hr at 40–50 °C and then diluted with 10 ml of acidified InstaGel (Packard, 7 ml N HCl in 100 ml InstaGel).

The peaks in the gels were separated at the locations indicated by the dashes perpendicular to the abscissa in Fig. 1. At each division, one half of the counts were added to the peak at the left, the other half to the peak on the right, regardless of the relative heights of the adjacent peaks.

All chemicals were analytical grade. H_2DIDS and $^3H_2$DIDS were prepared as described by Lepke et al. (1976). Chymotrypsin was from Boehringer, Mannheim.

Mathematical Methods

All model equations have been fitted to the experimental data by nonlinear least squares procedures. For the fits a computer routine (IMSL, 1980) based on the Levenberg-Marquardt algorithm (Brown & Dennis, 1972) has been used. For the one-state model (Table 1) identical results were obtained with the mentioned algorithm and a modified gradient method (Fletcher & Powell, 1963).

Each experiment yields three sets of data, pertaining to the time course of (i) unilateral attachment to the 60 K segment, (ii) unilateral attachment to the 35 K segment; and (iii) the reconstitution of band 3. Curve fitting of the three corresponding equations to the data was performed simultaneously using the appropriate mathematical model. Thus three sets of different data provide a single set of rate constants that pertains to a given model (Tables 2 and 5).

The accuracy of the fitted rate constants was insensitive to changes of pH; however, the accuracy with which the individual parameters at a given pH could be determined differed considerably. The residual sum of the least squares changed by not more than $\pm 1\%$ and the graphical representations of the model equations for the two-states model were not visibly modified when variations of the numerical values of the parameters k_0 or k_3 were less than $\pm 2\%$. Similar results were obtained when k_1 was varied by less than $\pm 10\%$, k_2 or k_{040} by less than $\pm 20\%$, or when k_{400} – the most uncertain parameter – was varied by 100% of the values specified in Table 5. These figures refer to the two-states model (Table 5, columns II). For the one-state model (Tables 2 and 5, columns I) the curve fitting routine gave estimates for the 95% confidence limits of the parameters. This leads to relative errors of approximately $\pm$ 25%, $\pm$30%, $\pm$80% and $\pm$20% of the numerical values in the table for k_0, k_1, k_2 and k_3, respectively. As in the two-states model, no pH dependence of the error limits could be detected.

Table 1. One-state model for cross-linking of the chymotryptic band 3 protein fragments of 60 K (*a*) and 35 K (*b*) by H_2DIDS (*s*) (Passow et al., 1982[a])

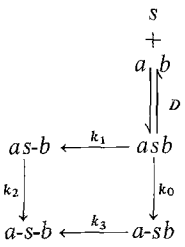

for $s \gg D$

$$\frac{a\text{-}sb}{\overline{AB}} = \frac{k_0}{k_0+k_1-k_3}\left(e^{-k_3 t} - e^{-(k_0+k_1)t}\right)$$

$$\frac{as\text{-}b}{\overline{AB}} = \frac{k_1}{k_0+k_1-k_2}\left(e^{-k_2 t} - e^{-(k_0+k_1)t}\right)$$

$$\frac{a\text{-}s\text{-}b}{\overline{AB}} = \frac{k_0}{k_0+k_1-k_3}\left(1-e^{-k_3 t}\right) + \frac{k_1}{k_0+k_1-k_2}\left(1-e^{-k_2 t}\right) - \left(\frac{k_0 k_3}{k_0+k_1-k_3} + \frac{k_1 k_2}{k_0+k_1-k_2}\right)\frac{1-e^{-(k_0+k_1)t}}{k_0+k_1}$$

[a] A hyphen,-, between *a* and *s*, or *b* and *s* indicates a covalent bond between H_2DIDS and site *a*, or site *b*, respectively. $D = ab \cdot s/asb = \text{const}$. The equations represent the changes with time of *a-sb*, *as-b* and *a-s-b* as derived from the one-state reaction scheme, assuming excess H_2DIDS in the bulk phase.

$AB = ab + asb + a\text{-}sb + as\text{-}b + a\text{-}s\text{-}b = $ total amount of band 3 chymotryptic fragments.

Results

Experimental Observations

The Time Course of Covalent Bond Formation and Cross-Linking in the presence of an Excess of H_2 DIDS in the Medium. When chymotrypsinized red blood cells are exposed to $^3H_2$DIDS, with increasing time, an increasing fraction of the originally, almost instantaneously bound $^3H_2$DIDS can no longer be removed from the cell surface by washing with albumin-containing buffer (Fig. 1). This indicates a transition from noncovalent to covalent binding to the membrane peptides. During this

Table 2. Rate constants in min^{-1} derived from least squares fits of the one-state model as defined in Table 1, and of the extended one-state model as defined in Table 3[a]

pH	k_0		k_1		k_2		k_3		k_4
	I	Ia	I	Ia	I	Ia	I	Ia	Ia
7.25	0.053	0.059	0.016	0.012	0.006	0.0010	0.0018	0.0012	0.014
7.36	0.085	0.092	0.024	0.022	0.0029	0.0012	0.0018	0.0013	0.012
7.40	0.095	0.102	0.026	0.010	0.077	0.014	0.0027	0.0029	0.014
7.90	0.17	0.182	0.046	0.043	0.0077	0.0039	0.0082	0.0065	0.031
8.01	0.17	0.190	0.085	0.045	0.090	0.0071	0.0063	0.0071	0.059
8.40	0.50	0.572	0.22	0.116	0.35	0.021	0.020	0.022	0.168
8.70	0.35	0.375	0.13	0.047	0.76	0.088	0.036	0.034	0.101
8.76	0.80	0.840	0.25	0.135	0.34	0.052	0.037	0.039	0.15

[a] I and Ia refer to the one-state and the extended one-state model, respectively. The original data for the experiments of pH 7.36 and 8.01 are presented in Figs. 2 and 6.

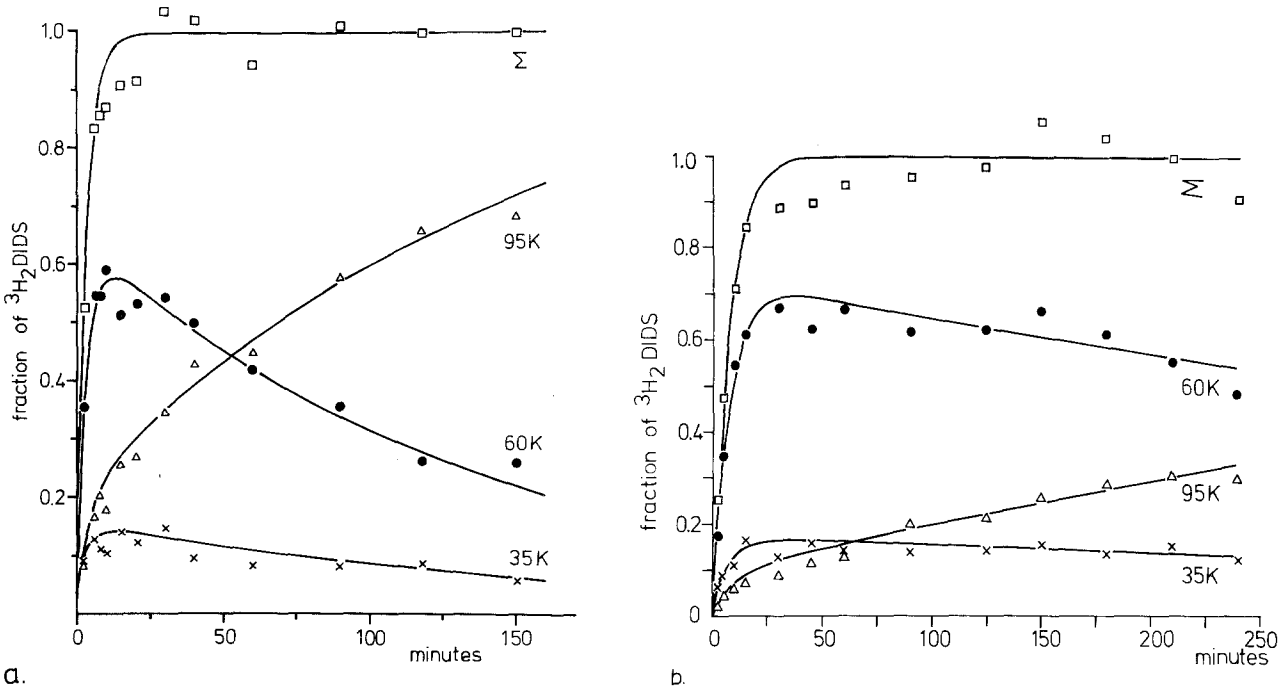

Fig. 2. Covalent $^3H_2$DIDS binding to the chymotryptic band 3 protein fragments and the formation of cross-links between them. Amounts of $^3H_2$DIDS bound covalently to the populations of 35 K, 60 K and 95 K, respectively, as functions of time. All other curves were calculated by means of the two-states model (Table 4). Curve denoted by Σ: sum of label in all peptides. Experiments were with intact cells. (*a*): Data taken from Fig. 1, pH 8.01. (*b*): Data obtained at pH 7.36. Ordinates: $^3H_2$DIDS binding as a fraction of total binding

process, the labeling profiles of SDS polyacrylamide gel electropherograms of the isolated membranes change considerably. Covalent binding is first detected on the 60 K and 35 K fragments of the band 3 protein. It increases with time and reaches maxima thereafter. The appearance of the maxima is related to the formation of a band that migrates at the same location as the original band 3 protein from red cells that had not been exposed to chymotrypsin. This newly formed band is the result of the establishment of cross-links in which the labeled 60 K and 35 K fragments become joined together with their unlabeled counterparts of 35 K and 60 K, respectively (Jennings & Passow, 1979).

The labeling of the various peptides can be determined quantitatively from labeling profiles such as those shown in Fig. 1. When the result of such determinations is plotted against time, curves like those represented in Fig. 2 are obtained. They confirm the conclusions drawn from the inspection of the labeling profiles and show that the 60 K fragment is labeled faster than the 35 K fragment.

Experiments of the type described were performed at several pH values in the range 7.25 to 8.75. Two examples are presented in Fig. 2*a* and *b*, which refer to pH 8.01 and 7.36, respectively. The curves show that the rates of covalent H_2DIDS binding to the 60 K and 35 K fragments as well as the rate of formation of the cross-linked product decrease considerably with decreasing pH.

Isolation of a Partial Reaction. In the experiments described above, the covalent bond formation was followed while the chymotrypsinized red cells were exposed to an excess of H_2DIDS in the medium. This ensures that throughout the time course of the experiment all H_2DIDS binding sites that have not yet undergone a covalent reaction with H_2DIDS remain occupied with noncovalently bound H_2DIDS.

The superimposition of the reactions that take place via the two pathways makes the analysis of the kinetics of cross-linking somewhat ambiguous. To reduce this ambiguity, we isolated one step of the cross-linking reaction from the others and traced it separately. We exposed the chymotrypsinized red cells to an excess of $^3H_2$DIDS at low pH (7.2) for a short time (10 min). Subsequently, the noncovalently bound H_2DIDS was removed by albumin washes. Under these circumstances, most of the H_2DIDS that remains attached to the red cells is covalently bound to the 60 K fragment. Resuspension in the absence of additional $^3H_2$DIDS permits one to follow the time course of the formation of the cross-link between the labeled 60 K fragments and the corresponding 35 K fragments without additional labeling of further 60 K frag-

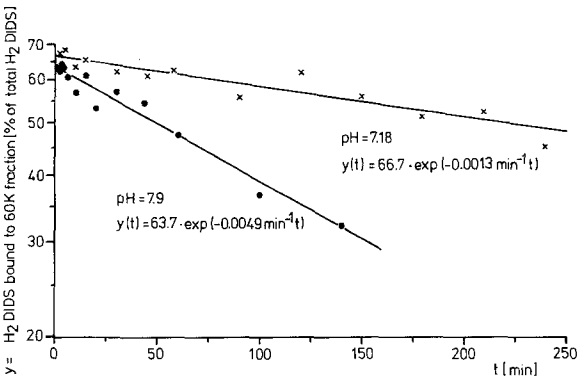

Fig. 3. Semilog plot of the time course of cross-linking at two different pH's. Measurements performed after covalent attachment of H_2DIDS to the 60 K chymotryptic band 3 protein fragment and removal of excess H_2DIDS. The figure shows the exponential decay of the 60 K segment. The straight lines were derived from nonlinear least squares fits. The rate constants correspond to k_3 as defined by the reaction scheme in Fig. 7. Experiments were with intact cells

ments by reversibly bound $^3H_2$DIDS. The time course of cross-linking now can be simulated by a single exponential (Fig. 3).

Figure 4*b* shows the pH dependence of the rate constant (designated k_3 in the reaction scheme in Fig. 7) as measured up to about pH 9.5 in intact red cells. Unfortunately, in intact red cells with increasing pH, the rate of pH equilibration decreases and the risk of hemolysis increases. For this reason the experiments could only be extended over a pH range up to about pH 9.5 (Fig. 4*b*). In experiments with resealed hemoglobin-free red cell ghosts (*see* Wood & Passow, 1981), this range could be extended to somewhat higher values. The adjustment of the pH is facilitated by the low buffer capacity of the ghosts, and the consequences of hemolysis are reduced since most of the H_2DIDS binding proteins of the red cell interior had been removed by the ghosting procedure. Essentially similar results were obtained with the ghosts as with the intact red cells. The data suggest that the reaction rate is governed by a single dissociating group with a pK of about 9.9–10.0 (Fig. 4*c*, *see below*).

For an assessment of the accuracy of the estimate of the pK value, it is necessary to describe the experiments and the mathematical evaluation in some more detail. Since the amount of work involved in the determination of the rate constants had to be kept within reasonable limits, each individual determination was based on a single data point. After attachment of H_2DIDS to lys *a* (*a-sb*) at pH 7.2, the cross-linking reaction (that leads to the formation of *a-s-b*) was permitted to proceed for a determined length of time at a range of pH values. Subsequently, the amount of $^3H_2$DIDS on the chymotryptic fragments that had not yet been cross-linked (*a-sb*(t)) was measured. The data points of three experiments with resealed ghosts are plotted in Fig. 4*a*. Each set of data points from the individual experiments was either fitted individually or all sets were fitted together by a nonlinear curve-fitting procedure to the equation: $a\text{-}sb(t)/(a\text{-}sb(t=0)) = \exp(-k_3 t)$, where $k_3 = \bar{k}_3/(1+10^{pK_r - pH})$. pK_r represents the pK value of *b* in *a-sb*, and $\bar{k}_3$ is a pH-independent rate constant.

The simultaneous fit of all data points yielded (with 95% confidence limits): $\bar{k}_3 = (0.421 \pm 0.100)\ min^{-1}$ and $pK_r = 10.04 \pm 0.16$. When the two data points with the highest pH values were omitted, we obtained: $\bar{k}_3 = 0.454\ min^{-1}$ and $pK_r = 10.09$. Thus, the results are not unduly dependent upon the measurements at the highest pH values. When each of the three experiments (with 7 data points each) is fitted independently, the three pairs of $\bar{k}_3$[min^{-1}] and pK_r are: 0.24, 9.75(△); 0.42, 10.05(○); and 0.48, 10.10(×). Two experiments with intact red cells that had enough data points for individual evaluations yielded for the pairs $\bar{k}_3$ and pK_r: 0.68, 9.95; 0.11, 9.25.

The data shown in Fig. 4*b* and *c* were obtained by replotting the individually determined values of k_3 against pH. The continuous curves were calculated using the values of $\bar{k}_3$ and pK_r obtained for the simultaneous fit of all data in Fig. 4*a* for the experiments with the ghosts (Fig. 4*c*) and of the values $\bar{k}_3 = 0.678\ min^{-1}$, $pK_r = 9.95$ for the experiments with the intact red cells (Fig. 4*b*).

Effect of Occupancy of the H_2DIDS Binding Sites on the Time Course of Cross-Linking. In the red cell membrane, the band 3 protein seems to exist predominantly in the form of dimers and tetramers (Steck, 1978; Dorst & Schubert, 1979; Nigg, Bron, Giradet & Cherry, 1980; Weinstein, Khodadad & Steck, 1980; Pappert & Schubert, 1981). This raises the question whether H_2DIDS binding to one protomer of a dimer or tetramer would affect the rate of cross-linking of the adjacent protomers.

To examine this question, two sets of experiments were performed. 1) Chymotrypsinized red cells were exposed to H_2DIDS at low pH (7.4) for varying lengths of time. At the end of these time periods, the cells were washed with albumin-containing media to remove reversibly bound H_2DIDS. In this manner batches of cells were obtained in which the occupancy of the 60 K fragments with unilaterally bound $^3H_2$DIDS varies. The various batches of cells were now incubated

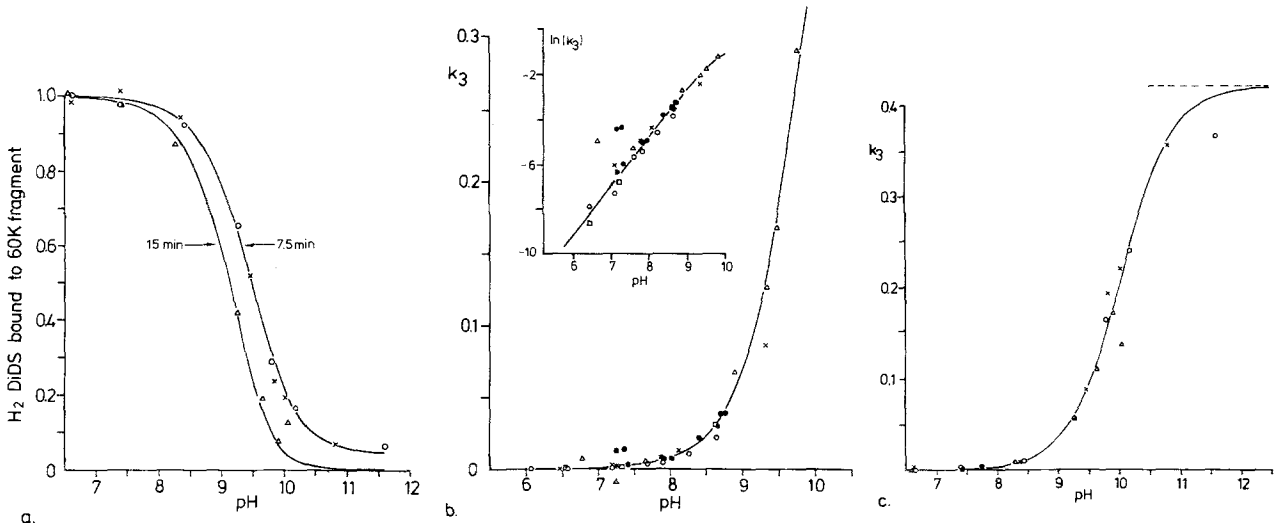

Fig. 4. pH dependence of cross-linking: After unilateral attachment to the 60 K segment, excess H_2DIDS is removed and cross-linking of the 60 K H_2DIDS fragment with the 35 K fragment is observed as function of time t. From this data, the rate constants used as ordinates for *b* and *c* have been calculated by means of the equation:

$a\text{-}sb(t)/a\text{-}sb(t=0) = \exp(-k_3 t)$, where t = cross-linking time and $k_3 = \bar{k}_3/(1+10^{pK_r - pH})$.

The continuous lines were calculated by a nonlinear curve fitting procedure. (*a*) pH dependence of cross-linking. After unilateral attachment to the chymotryptric 60 K segment, excess $^3H_2$DIDS is removed and cross-linking of the 60 K fragment with the 35 K fragment is observed. Plotted in the figure is the $^3H_2$DIDS associated with the 60 K fragment (that carries lys *a*) as measured after $t=7.5$ min (o, ×) or $t=15$ min (Δ) of cross-linking, at the pH values indicated on the abscissa. The ordinate of the figure represents $a\text{-}sb(t)/a\text{-}sb(t=0)$. The data are from three different experiments with resealed white ghosts. The curves are the result of a simultaneous least squares fit which yields a single pair of $\bar{k}_3$ and pK_r (0.421 min^{-1} and 10.04, respectively), used to calculate the curves in the figure. Instead of the expected three curves, only two are shown, since the fitted curves for the data points designated by o and × happen to coincide. From each data point in this panel, the value for k_3 can be calculated by means of the equation presented above. The values are plotted in *c*. (*b*): Rate constant k_3 as function of pH. Derived from experiments with intact erythrocytes. Same experimental arrangement as in *a*. Continuous line calculated from $\bar{k}_3 = 0.678$ min^{-1} and $pK_r = 9.95$. • designates k_3 values derived from the time course of curves like those in Fig. 2*a* and *b* by the use of the extended one-state model or the two-states model (Both types of evaluations yield virtually indistinguishable results: *see* Tables 2 and 5). *Ordinate:* k_3 in min^{-1}. *Abscissa:* pH. *Inset:* Same data, but replotted on logarithmic scale. (Three points with $k_3 < 0$ have been omitted). Ordinate: ln (k_3). Abscissa: pH. (*c*): Rate constants k_3 as function of pH. Experiments were with resealed ghosts. Same data as in *a*. The drawn curve was calculated for $\bar{k}_3 = 0.421$ min^{-1} and $pK_r = 10.04$

at elevated pH in H_2DIDS-free media and the rate of cross-linking was followed. With increasing occupancy of the H_2DIDS binding sites, there is an increase of the probability of the presence of more than one unilaterally bound H_2DIDS molecule per dimer or tetramer of band 3. Nevertheless, the rate of cross-linking was always the same. Thus, these experiments (not documented) yielded no evidence for interactions between the H_2DIDS binding sites on band 3 molecules that are constituents of dimers or tetramers.

2) Similar conclusions could be drawn from another set of experiments. Chymotrypsinized red cells were first incubated for 1 min at low pH (7.4) in a medium that contained labeled H_2DIDS at a concentration of 10 μM. Within the time alotted, this leads to covalent bond formation with the 60 K fragments of some 10% of the band 3 molecules per cell. After removal of the noncovalently bound $^3H_2$DIDS by albumin washes, the cells were separated into two batches. One was resuspended in a medium that contained a large excess of nonradioactive H_2DIDS that leads to the occupancy of all H_2DIDS binding sites available. The other was resuspended in a H_2DIDS-free medium. Thus, in the second batch, most $^3H_2$DIDS molecules are bound to band 3 molecules whose nearest neighbors are unoccupied, while in the first batch each $^3H_2$DIDS molecule is bound to a band 3 molecule whose nearest neighbors are occupied. The rates at which the 60 K fragments were cross-linked with their 35 K counterparts were found to be indistinguishable regardless of whether nonradioactive H_2DIDS was present or not. This result supports the conclusion that interactions between the constituents of band 3 dimers or tetramers are negligi-

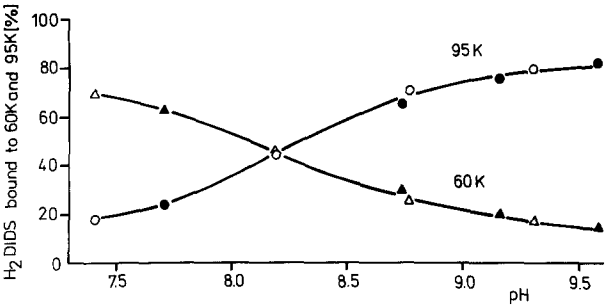

Fig. 5. Effect of H_2DIDS on the rate of cross-linking by $^3H_2$DIDS. After unilateral attachment of $^3H_2$DIDS to the 60 K chymotryptic segment of band 3 protein (incubation for 1 min at 37 °C, pH 7.2 and subsequent removal of unreacted $^3H_2$DIDS), cross-linking was allowed to proceed in the absence (open symbols) or presence (filled symbols) of an excess of nonradioactive H_2DIDS at 37 °C during a 60-min incubation period at different pH's. The emerging 95 K cross-linked protein and the residual 60 K fraction are represented as percentages of the sum of $^3H_2$DIDS on all fractions 35 K, 60 K and 95 K

ble, at least as far as the cross-linking reaction is concerned (Fig. 5).

Comparison of Experimental Data with Mathematical Models of the Cross-Linking Reaction

The One-State Model. The simplest scheme that can be visualized for the cross-linking reaction is presented in Table 1 (Passow et al., 1982). Covalent bond formation of the H_2DIDS molecule (*s*) may take place along two different reaction pathways. Either the noncovalently bound H_2DIDS (*asb*) binds covalently first to a specific amino acid residue *a* on the chymotryptic 60 K fragment to form *a-sb* and subsequently links this fragment by a further covalent bond to another amino acid residue *b* on the chymotryptic 35 K fragment. Alternatively, H_2DIDS combines covalently first with *b* to yield *as-b* and then continues to establish cross-links by covalent reaction with *a*. The final result of both reaction sequences is the reconstitution of a band at the 95 K location on the polyacrylamid gels (*a-s-b*). An extension of the model ("extended one-state model") includes as an additional reaction pathway the transition $asb \rightarrow a\text{-}s\text{-}b$, i.e., the assumption that there exists a finite probability for the simultaneous reaction of *a* and *b* with the two isothiocyanate residues of the same H_2DIDS molecule *s*.

From the reaction scheme in Table 1 a set of three equations can be derived that describes the changes with time of *a-sb*, *as-b* and *a-s-b* in terms of the one-state model. Nonlinear least squares fits of these equations to the experimental data, as shown in Fig. 2*a* and *b*, yield the parameter values in Table 2 denoted by I. At all pH values, the rates of reaction with *a* (rate constant k_0) exceed those with *b* (rate constant k_1) by a factor of about 3. Unilateral binding to *a* takes place more than one order of magnitude faster than the subsequent cross-linking (rate constants k_3). In contrast, the initial binding to *b* takes place at a higher rate than the subsequent cross-linking when the exposure to H_2DIDS is performed at low pH.

There exist systematic deviations between the one-state model and the experimental observations. Similar to the experiments depicted in Fig. 6*a* and *b*, in the majority of the other experiments, the computer fits yield curves for the time courses of the formation of *as-b* (i.e., covalent H_2DIDS binding to *b*) that overshoot the actually observed data points at the beginning and later decay too rapidly. Furthermore, the rate of formation of the cross-link (*a-s-b*) is underestimated during the initial phase. In contrast, the time course of appearance and decay of *a-sb* is nearly always reasonably well represented. The quality of the fit improves considerably when the data are fitted to the extended one-state model that permits the additional reaction $asb \rightarrow a\text{-}s\text{-}b$ (Table 2). The rate constants k_0 and k_3, as defined by this extended model, have very similar numerical values as the corresponding constants defined by the original version of the one-state model. The other rate constants do change such that k_2 and k_3 on the one hand and k_1 and k_4 on the other become indistinguishable.

The Two-States Model. Since a simultaneous reaction of *a* and *b* with *s* should be a very rare event, and hence may not represent the most plausible explanation of the deviations from the one-state model, we considered other possible extensions of that model. As in the original one-state model, interactions between the H_2DIDS binding sites on adjacent band 3 molecules are neglected, but it is assumed that in each band 3 molecule *a* and *b* may exist in two different conformeric states, called *a** and *b**, respectively with different reactivities towards the SCN-groups of H_2DIDS. The ensuing reaction network is depicted in Fig. 7.

The network contains more independent parameters than can safely be determined from the experimental data. To find a simpler, but still adequate and meaningful representation of the data, constraints had to be imposed on this model.

Several special cases were investigated (*see below*) but none of them proved to be satisfactory

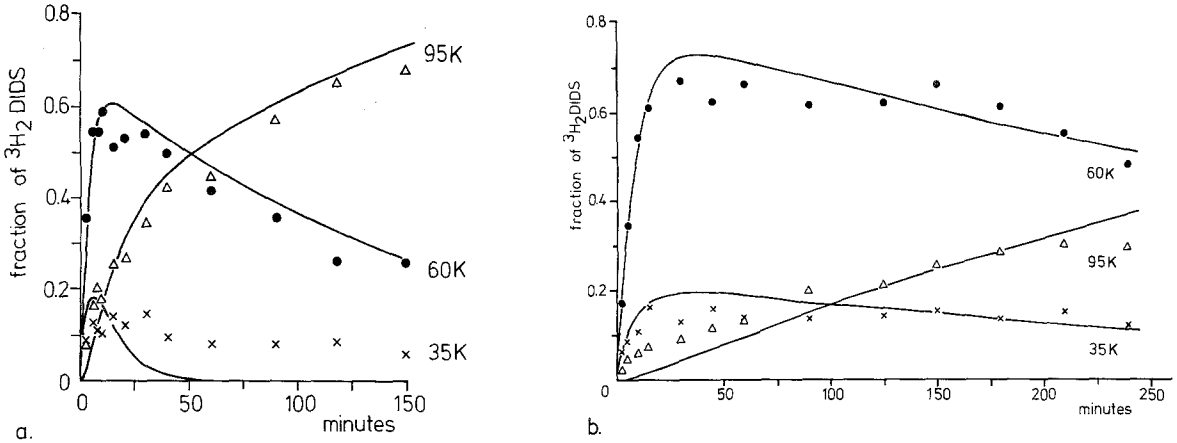

Fig. 6. Time course of cross-linking: fit of the one-state model (Table 1) to experimental data. (*a*): pH 8.01; same data as in Fig. 2a. (*b*): pH 7.36; same data as in Fig. 2b

Table 3. Extended one-state model[a]

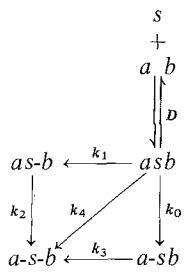

for $s \gg D$

$$\frac{a\text{-}sb}{\overline{AB}} = \frac{k_0}{k_0+k_1+k_4-k_3}\left(e^{-k_3 t} - e^{-(k_0+k_1+k_4)t}\right)$$

$$\frac{as\text{-}b}{\overline{AB}} = \frac{k_1}{k_0+k_1+k_4-k_2}\left(e^{-k_2 t} - e^{-(k_0+k_1+k_4)t}\right)$$

$$\frac{a\text{-}s\text{-}b}{\overline{AB}} = 1 - \frac{k_0}{k_0+k_1+k_4-k_3}e^{-k_3 t} - \frac{k_1}{k_0+k_1+k_4-k_2}e^{-k_2 t} - \left(1 - \frac{k_1}{k_0+k_1+k_4-k_2} - \frac{k_0}{k_0+k_1+k_4-k_3}\right)e^{-(k_0+k_1+k_4)t}$$

[a] The symbols have the same meaning as in Table 1

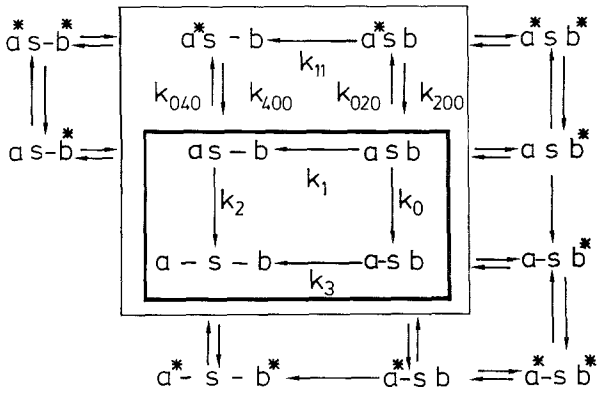

Fig. 7. Reaction scheme for a four-states model for cross-linking by H_2DIDS, assuming two conformeric states for each *a* and *b* (designated by presence or absence of *), with different reactivities towards H_2DIDS. Large box: The most general subsystem that has been investigated quantitatively. A special case of this subsystem that assumes $k_{11}=0$ and equilibrium between *asb* and *a*sb*, is called "two-states model" (Table 4). It represents a simple reaction scheme that yields an acceptable fit to the experimental observations. Small box: "one-state model" as presented in Table 1. (The dissociation equilibria $s+ab \rightleftharpoons asb$, $s+a^*b \rightleftharpoons a^*sb$, etc., have been omitted)

except one subsystem called the "two-states model" (Kampmann, Lepke, Fasold & Passow, 1982). This model is delineated by the large box in Fig. 7. It comprises the one-state model discussed in the preceding section as a subsystem (heavy lined box in Fig. 7). It rests on the simplifying assumption that the H_2DIDS binding site may exist in two different states, one (called *ab*) in which thiocyanylation of either *a* or *b* may occur and another one (called *a*b*) in which neither *a* nor *b* can react. This is equivalent to the statement that all *k*'s that are explicitly defined in Fig. 7 are finite except k_{11} which is zero. It is further stipulated that transitions between *ab* and *a*b* are still feasible when *s* becomes noncovalently bound ($asb \rightleftharpoons a^*sb$) or covalently attached to *b* ($as\text{-}b \rightleftarrows a^*s\text{-}b$). In addition it is postulated that the former reaction is fast enough to lead to the establishment of an equilibrium which can be defined by a mass law constant, while the latter is much slower and requires the

Table 4. Reaction scheme and equations predicting the variations with time of $a\text{-}sb/\overline{AB}$, $(as\text{-}b+a^*s\text{-}b)/\overline{AB}$ and $a\text{-}s\text{-}b/\overline{AB}$ for the two-states model as used for the final evaluation of the experiments[a]

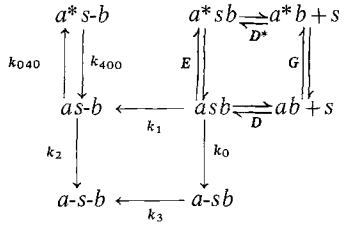

equilibria:

$$\frac{a^*sb}{asb}=E,\quad \frac{a^*b}{ab}=G,\quad \frac{ab\cdot s}{asb}=D,\quad \frac{a^*b\cdot s}{a^*sb}=D^*,\quad G\cdot D=D^*\cdot E$$

boundary conditions and mass balance:

$a\text{-}sb=a\text{-}s\text{-}b=as\text{-}b=a^*s\text{-}b=0 \quad \text{for } t=0$

total mass $=\overline{AB}=$const.

$$\overline{AB}=asb(t=0)+a^*sb(t=0)+ab(t=0)+a^*b(t=0)=asb(t=0)\cdot(1+E+(1+G)\,D/s)=asb(t=0)\cdot(k_0+k_1)/\delta$$

s independent of time t

$$\frac{a\text{-}sb}{\overline{AB}}=\frac{\delta k_0}{(k_0+k_1)(k_3-\delta)}\left[e^{-\delta t}-e^{-k_3 t}\right]$$

$$\frac{as\text{-}b+a^*s\text{-}b}{\overline{AB}}=\frac{\delta k_1}{k_0+k_1}\left[\frac{k_{040}+k_{400}-\delta}{(\psi_1-\delta)(\psi_2-\delta)}\,e^{-\delta t}-\frac{1}{k_{400}(\psi_1-\psi_2)}\left(\frac{\psi_2(\psi_1-k_{400})}{\psi_1-\delta}\,e^{-\psi_1 t}-\frac{\psi_1(\psi_2-k_{400})}{\psi_2-\delta}\,e^{-\psi_2 t}\right)\right]$$

$$\frac{a\text{-}s\text{-}b}{\overline{AB}}=\frac{\delta}{k_0+k_1}\left[\frac{1}{\delta}\left(\frac{k_0k_3}{k_3-\delta}+\frac{k_1k_2(k_{400}-\delta)}{(\psi_1-\delta)(\psi_2-\delta)}\right)(1-e^{-\delta t})-\frac{k_0}{k_3-\delta}\,(1-e^{-k_3 t})\right.$$
$$\left.+\frac{k_1k_2}{\psi_1-\psi_2}\left(\frac{k_{400}-\psi_1}{\psi_1(\psi_1-\delta)}\,(1-e^{-\psi_1 t})-\frac{k_{400}-\psi_2}{\psi_2(\psi_2-\delta)}\,(1-e^{-\psi_2 t})\right)\right]$$

where

$$\delta=(k_0+k_1)/(1+E+(1+G)\,D/s)=(k_0+k_1)/(1+D/s+(1+D^*/s)\,E)$$

$$\psi_{1,2}=(k_2+k_{040}+k_{400})/2\pm\sqrt{((k_2+k_{040}+k_{400})/2)^2-k_2k_{400}}$$

i.e. $\psi_1+\psi_2=k_2+k_{040}+k_{400}$; $\psi_1\psi_2=k_2k_{400}$.

6 independent parameters, e.g., k_0/k_1, δ, k_2, k_3, k_{040}, k_{400}

[a] $\overline{AB}$ = total amount of all forms, i.e. the two chymotryptic band 3 protein fragments and the 95 K product of the cross-linking reaction

consideration of the backward and forward rate constants individually. The equations describing this model are summarized in Table 4.

If one takes into account that under our experimental conditions the concentration of H_2DIDS in the medium is always large enough to saturate all H_2DIDS binding sites (i.e., $s \gg D^*, D$), the equations for the two-states model contain six independent parameters (*see* Table 4). It is evident from the figure in Table 4 that the three parameters k_0, k_1 and $E=a^*sb/asb$ are not independent of one another. Since there is no independent information available about the equilibrium $asb \rightleftharpoons a^*sb$, one can only determine the ratio k_0/k_1 but not the individual values of these rate constants. For the present purpose, k_0 and k_1 were calculated individually by arbitrarily setting $E=0$. Whenever experimental estimates of E should become available, the absolute values of k_0 and k_1 can be calculated from the equations in Table 4.

The drawn curves in Fig. 2*a* and *b* provide examples for the fit of the two-states model specified above to the time course of H_2DIDS binding at pH 8.0 and pH 7.4, respectively. The fits to similar experiments that had been performed at other pH values are as reasonable as those for the experiments shown in this figure (Table 5).

The values for the various parameters derived from the fits are listed in Table 5 (Columns II). They show that k_0, k_1 and k_3 are rather similar

Table 5. Rate constants in min^{-1} derived from least squares fits of the one-state model (Table 1) and the two-states model (Table 4)[a].

pH	k_0		k_1		k_0/k_1		k_2		k_3		k_0/k_3		k_{400}	k_{040}	k_{040}/k_2
	Model I	Model II	I	II	I	II	I	II	I	II	I	II	II	II	II
7.25	0.053	0.059	0.016	0.025	3.3	2.4	0.006	0.43	0.0018	0.0012	29	49	0.0010	0.34	0.79
7.36	0.085	0.092	0.024	0.034	3.5	2.7	0.0029	0.53	0.0018	0.0013	47	72	0.0033	0.96	1.81
7.40	0.095	0.101	0.026	0.031	3.7	3.3	0.077	1.35	0.0027	0.0025	36	40	0.026	1.0	0.74
7.90	0.17	0.18	0.046	0.073	3.7	2.5	0.0077	0.26	0.0082	0.0065	21	27	0.0050	0.28	1.08
8.01	0.17	0.19	0.085	0.11	2.0	1.7	0.090	0.91	0.0063	0.0072	27	28	0.0105	0.64	0.70
8.40	0.50	0.57	0.22	0.29	2.3	2.0	0.35	40	0.020	0.0215	25	27	0.037	28	0.70
8.70	0.35	0.39	0.13	0.15	2.7	2.5	0.76	0.8	0.036	0.038	10	10	0.0003	0.2	0.25
8.76	0.80	0.84	0.25	0.28	3.2	3.0	0.34	1.9	0.037	0.0388	22	23	0.081	1.4	0.74
white ghosts:															
7.94	0.13	0.14	0.044	0.055	3.0	2.5	0.020	0.25	0.0036	0.0034	36	40	0.012	0.33	1.29

[a] I and II refer to the one-state model and the two-states model, respectively. The original data at pH 7.36 and 8.01 are presented in Figs. 2 and 6. Except for one experiment (lowest line in the table) all experiments were performed with intact cells.

to the corresponding rates that can be derived from the one-state model. k_0 and k_3 are almost indistinguishable from the corresponding constants of the extended one-state model. Moreover, the numerical values of k_3 derived from the computer fits of all three models are rather similar to the independent determinations of this rate constant in the isolated reaction *a-sb* → *a-s-b* (Fig. 4*b* and *c*). In the one-state model, as well as in the two-states model, the initial increase of *a-s-b* with time should show a lag period. This does not appear in the data and was one of the reasons that led us to abandon the simplest form of the one-state model. Nevertheless, in the two-states model, the drastically higher value of k_2 reduces this lag period to a negligible time span and accounts for the observed rapid increase of *a-s-b*. The additional degree of freedom introduced by the incorporation of the transition *as-b* ⇄ *a*s-b*, nevertheless, allows a much better fit of the data. The rapid formation of *a*s-b* (rate constant k_{040}) and the slow reconversion of that form into *as-b* fragment (rate constant k_{400}) accounts for the rapid appearance of the labeled 35 K fragment and the protracted time course of its disappearance. It should be noted that in this model the ratio of the rate constants at the branching point of the reaction sequence:

*a*s-b*
↑↓
as-b ← *asb*
↓
a-s-b

are reasonably well defined (e.g., k_{040}/k_2), while the individual values show a considerable scatter. This holds particularly for k_{040} and k_{400}. Nevertheless, it is obvious that k_{040} and k_{400} are of different orders of magnitude and that the equilibrium constant k_{040}/k_{400} is large and hence favors the formation of *a*s-b*.

In view of the inaccuracies mentioned above, it should be emphasized that the fits are quite sensitive to small modifications of the model. This is due to the fact that the factors and the exponents in the equations in Tables 1 and 2 each contain several different specific combinations of the same independent parameters. Thus, in contrast to a simple series expansion with six coefficients, the model imposes powerful constraints that reduce the degrees of freedom for the fit of the parameters.

There are simple criteria that help to judge whether or not a given modification of the models yields a meaningful fit. If the number of independent parameters is increased above 6, the fits do not improve much, while the numerical values for the parameters may now include several ones that are meaningless, e.g., negative or smaller than 1.0 in cases where the model requires values greater than 1.0. This indicates that the scatter of the data limits the resolution. If the number of independent parameters is reduced to below 6, then the equations of the two-states model degenerate to expressions that are *formally* identical with those for the one-state model and hence do not fit the data accurately. This occurs, for example, if one postulates that the reversible reaction *as-b* ⇄ *a*s-b* proceeds much faster than the transition *as-b* → *a-s-b* and hence is always at equilibrium. In this case the predicted time course is formally identical to that of the one-state model, in which k_2 has to be replaced by $k_2/(1+F)$, (where $F = a^*s\text{-}b/as\text{-}b$), and *as-b* by *as-b* + *a*s-b*. Another special case,

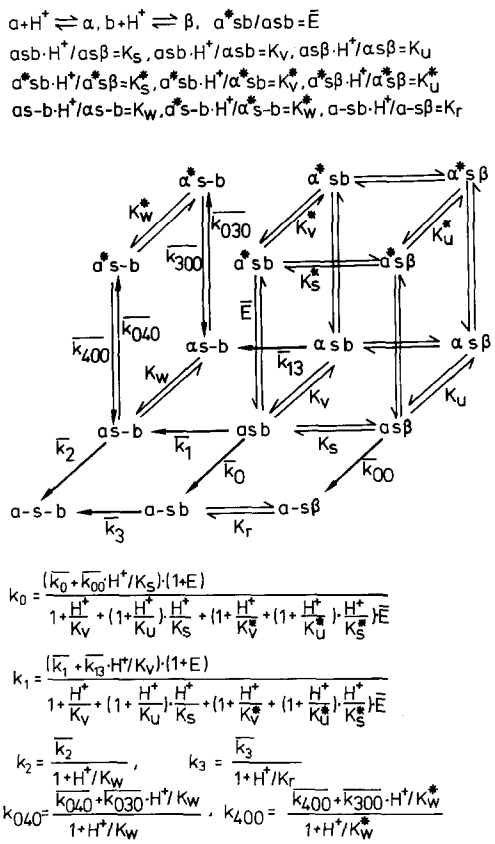

Fig. 8. Hydrogen ion equilibria at the H_2DIDS binding site *ab*. The pH-dependent rate constants k_0, k_1, k_2, k_3 of the two-states model (Table 4) are expressed as functions of the pH-independent rate constants $\bar{k}_0$, $\bar{k}_1$, $\bar{k}_2$, $\bar{k}_3$, the mass law constants $\bar{E}=a^*sb/asb$ and the hydrogen ion dissociation constants K_r, K_s,... . $E=(a^*sb+\alpha^*sb+a^*s\beta+\alpha^*s\beta)/(asb+\alpha sb+as\beta+\alpha s\beta)$. Note that *asb* and *a*sb* in this figure have meanings different from those in Table 4 where no distinction has been made between the various protonated and deprotonated forms in which *asb* and *a*sb* may exist. In the present figure, in contrast to Table 4, *a*sb* and *asb* refer only to the two states of the completely deprotonated form of the H_2DIDS binding site Corresponding expressions for the rate constants k_0, k_1... for the extended one-state model are obtained if one sets $E=\bar{E}=0$ in the equations above and replaces the expressions for k_{040} (pH) and k_{400}(pH) by $k_4=\bar{k}_4/(1+H^+/K_v+(1+H^+/K_u)H^+/K_s)$ which yields simple relations between k_0/k_4, $\bar{k}_0/\bar{k}_{00}$, pK_s and between k_1/k_4, $\bar{k}_1/\bar{k}_{13}$, pK_v

where $k_{11}=k_1$, $k_{040}=k_{020}$, $k_{400}=k_{200}$ (*see* Fig. 7) also yields no adequate representation of the data.

pH Dependence. Previous work of Ship et al. (1977) had shown that the rate of covalent binding of H_2DIDS increases with increasing pH. Our data confirmed this observation and indicated that all rate constants that are required to describe the cross-linking reaction show that increase. This is to be expected if the cross-link is to be established between lysine residues.

Unfortunately, an unambiguous analysis of the pH dependence of most of the various rate constants encounters difficulties. The reason is that the hydrogen ion equilibria at lys *a* and lys *b* enter the rate equations in various combinations which, given the scatter of the data, cannot be resolved statisfactorily. The complexity of the situation is illustrated for the two-states model in Fig. 8, but it is easy to visualize that the effects of varying the pH are still fairly complex in the two simpler models. Thus, it was not possible to determine the pertinent pK values, with the exception of pK_r, the pK value that pertains to the rate constant k_3, describing the transition *a-sb* → *a-s-b*.

Evaluation of the data in terms of all three models considered above yielded k_3 values that are rather similar (*cf.* Table 2 and 5). They agree reasonably well with the k_3 values determined by measuring the rate of the isolated reaction (*see* p. 203). The least squares fit to the equation $k_3=\bar{k}_3(1+10^{pK_r-pH})$ yields $\bar{k}_3=0.143\pm0.091$ (min^{-1}) and $pK_r=9.19\pm0.37$ for the extended one-state model, and $\bar{k}_3=0.17\pm0.13$ (min^{-1}) and $pK_r=9.25\pm0.44$ for the two-states model. These figures have to be compared to $\bar{k}_3=0.42\pm0.10$ (min^{-1}) and $pK_r=10.04\pm0.16$ derived from the independent determination of the isolated reaction (*see* p. 204 and Fig. 4*c*).

In the curve fitting procedures used so far, the sum of the squares of the absolute errors between data and model function had been minimized. This tends to place more emphasis on data points that have large absolute values than on data points that have low absolute values. This affects the analysis of the pH dependence of the k_3 values insofar as it places more weight on the determinations at high pH than on those at low pH. We have, therefore, evaluated the data also by minimizing the relative errors, whereby the weight of the individual errors becomes independent of the abolute values of the data. The results of such evaluation of the data for the isolated reaction *a-sb* → *a-s-b* are virtually indistinguishable from those obtained by using absolute errors. k_3 is now 0.361 instead of 0.421 (min^{-1}) and $pK_r=10.1$ instead of 10.04. The parameters derived from the time course of the cross-linking reaction now assume the values $\bar{k}_3=0.133$, $pK_r=9.18$ for the extended one-state model and $k_3=0.595$, $pK_r=9.89$ for the two-states model. These values deviate somewhat from those of the corresponding fits based on the minimalization of the squares of the absolute errors that are listed in the preceding paragraph. Nevertheless, it seems clear that regardless of the criteria used for defining the error, the results derived from the time

course of cross-linking are compatible with those derived from the isolated reaction, and that the latter is governed by a pK value of about 10.

Concluding Remarks. The determinations of the label on the 35 K band is subject to greater error than the determination of the label on the 60 K band or the reconstituted 95 K band. This raises the question as to what extent our results could be affected by H_2DIDS binding to the 35 K region that does not lead to cross-linkage, or only at very high pH. For the evaluation of the time course of the cross-linking reaction, the behavior of the $^3H_2$DIDS in the 35 K region is indeed taken into account. However, it does by no means rest exclusively on this behavior, since the computer executes a simultaneous fit to all three bands, the 35 K band, the 60 K band and the reconstituted 95 K band. The deviations from the one-state model that led to the theoretical work described above is easily apparent when one only considers the time course of appearance of the reconstituted 95 K band. Moreover, the independent determinations of the rate constant k_3 rest entirely on the disappearance of the 60 K band. In addition, this rate constant is determined by a single exponential, and the pH dependence can be fitted by a single pK value. All this suggests that the reaction that is pertinent for the present work takes place at a single NH_2 group on the 35 K segment of the band 3 protein. Nevertheless, the existence of some additional H_2DIDS binding groups in the 35 K region cannot definitely be excluded until the H_2DIDS binding sites along the peptide chain have been established by biochemical methods. A model that takes such groups into account yields a fit inferior to that of the models considered here, as we observed in a computer simulation.

Discussion

Two Conformational States of the H_2DIDS Binding Site

The simplest possible model for the formation of the cross-link between the two lysin-residues *a* and *b* is represented by a branching reaction: the reversibly bound H_2DIDS molecule *s* reacts first either with lys *a* (*asb* → *a-sb*) or with lys *b* (*asb* → *as-b*) before the cross-link (*a-s-b*) is established. The main conclusion that we draw from our experimental observations is that the cross-linking reaction shows deviations from this behavior and that the deviations can be interpreted with equal accuracy by at least two different models. One, the "extended one-state model," requires that the reversible H_2DIDS binding leads to a fixation of the inhibitor molecule such that the rate of reaction with the two lysine residues *a* and *b* is determined by the oscillations of these residues rather than by the oscillations of the H_2DIDS molecule. This would account for the possibility that, in addition to the two modes of unilateral attachment of the H_2DIDS molecule (either first to lys *a* or first to lys *b*) a simultaneous attachment at both isothiocyanate groups with lys *a* and lys *b* may take place. The numerical value of k_4 that describes the probability for this simultaneous attachment is of the same order of magnitude as the numerical values of the rate constants k_0 and k_1 which indicate the probabilities for the unilateral attachment to *a* or *b*, respectively. Thus, the actual occurrence of a simultaneous attachment has a much higher probability than one would expect for a reaction with independently oscillating lysine residues. To make the model acceptable from the point of view of chemical kinetics, one would need to postulate, therefore, that the movements of lys *a* and lys *b* are partially coupled or, more plausibly, that the H_2DIDS binding site may exist in two distinct conformations, one in which the two residues oscillate independently and another in which their movements are rigidly coupled and thus give rise to a simultaneous reaction with the two isothiocyanate groups of the H_2DIDS molecule. The sum of the squares of errors for this model is virtually identical with the sum of the squares of the errors for the other model, that we call the "two-states model" (Table 6). In this latter model the assumption made is that the lysine residue *a* may exist in two states, exposed or buried, and that only the depro-

Table 6. Sum of least squares for the computer fits to the extended one-state model (Ia) and the two-states model (II)

pH	Ia[1])	II[1])	Ia[2])	II[2])
7.25	21.1	21.0	1.020	0.000
7.36	4.6	4.6	0.402	0.372
7.40	1.8	1.8	0.770	–[a]
7.90	7.0	6.9	1.100	0.856
8.01	14.9	14.3	0.403	0.338
8.40	34.1	34.2	0.610	0.677
8.70	73.5	73.4	7.30	7.22
8.76	5.5	5.5	5.79	–[a]

[1] and [2] refer, respectively, to fits in which the squares of the absolute or relative deviations between data and model function have been minimized

[a] Overflow. These two data points have been omitted in the calculations of k_3 and pK_r on p. 210.

tonated form of lys *a* may exist in the buried state. The former model accounts particularly well for the initial high rate of cross-linking that exceeds the rate predicted by other models in which the closing of the crosslink may take place only after preceding unilateral reactions, e.g., the formation of *a-sb* or *as-b*. The scatter of the data makes it impossible, however, to detect or exclude the S-shape of the curves predicted by these other models for *a-s-b* as a function of time[1]. For the two-states model, six parameters need to be fitted. However, at the bifurcation of the reaction scheme that follows the formation of *as-b*, one can only determine the ratios of the various rate constants, e.g. k_2/k_{040}, with any degree of certainty, while the individual values show a considerable scatter. The other model, that permits simultaneous reactions of *a* and *b* with the two isothiocyanate groups of H_2DIDS requires only five parameters, all of which are well defined. A comparison of the residual error sums between the two models (Table 6) shows that the sums are essentially identical.

Thus, for the time being, we must be content with the conclusion that the one-state model is clearly insufficient, that possible alternatives can be formulated, but that solely on the basis of the information that can be derived from the kinetics of cross-linking, a final decision between the two proposed extensions of the one-state model is not yet possible. It may also be noted that the two models are not mutually exclusive. In fact, a combination of them could be expected to yield an even better description of the time course of the cross-linking reaction than each model alone, and thus provide a single and relatively simple picture about the behavior of the two lysine residues at the H_2DIDS binding site.

The meaning of the various rate constants depends on the model that defines them. However, the reaction *a-sb* → *a-s-b* that defines k_3 can be isolated and studied free of hypothetical assumptions about the reaction sequence for the cross-linking reaction as a whole.

All three models, including the simple one-state model, yield k_3 values that agree fairly well amongst each other and with the values obtained for the independently measured value of the isolated reaction. Thus, one may conclude that this step in the reaction sequence is well defined.

All three models also agree that the unilateral binding of *s* to *a* (*asb* → *a-sb*) is faster than the unilateral binding to *b* (*asb* → *as-b*). The numerical values of the ratios k_0/k_1 are independent of pH and amount to 3.0, 2.5 and 5.6 for the one-state, two-states and the extended one-state model, respectively. They also agree that the unilateral attachment to *a* (*asb* → *a-sb*) is much faster than the subsequent cross-linking reaction *a-sb* → *a-s-b*. They disagree with the interpretation of the other branch of the reaction scheme that leads from *asb* to *a-s-b*. The direct transition *asb* → *a-s-b* or the combination of the storage by isomerization of *as-b* ⇄ *a*s-b* and the high rate of reaction of *as-b* → *a-s-b* account for the deviations from the one-state model. Thus, we may conclude that the reaction sequence *asb* → *a-sb* → *a-s-b* is well established while the transition *asb* → *a-s-b* via the other branch of the reaction sequence exhibits additional features that are not yet understood, but can possibly be explained by one or both of the extensions of the one-state model described above.

Regardless of the specific nature of the reaction pathway that accounts for the kinetics of the cross-linking reaction, it is obvious that the deviations from the simple one-state model requires the assumption that the H_2DIDS binding site may exist in at least two distinct conformational states and that the transition from one of these states to the other is associated with changes of the reactivity of lys *a* or lys *b*, or both.

The existence of two conformeric states of the H_2DIDS binding site had been postulated previously on the basis of independent pieces of evidence. Most directly bearing on the present results is the work of Passow et al., 1980*b*, on the rate of dinitrophenylation of lys *a*. This lysine residue can be fairly selectively dinitrophenylated. This leads to an inhibition of anion transport and a corresponding reduction of the capacity of H_2DIDS to bind covalently to the 60 K segment of band 3. The rate of the reaction of N_2ph-F with *a* can be influenced by the presence of substrates or inhibitors of anion transport. Increasing the concentration of the substrate Cl^- enhances the rate of reaction, suggesting that the combination of Cl^- with the substrate binding site shifts an equilibrium between two forms of *a* with different reactivities towards the form with the higher reactivity. Ca^{++} inhibits anion transport at the

[1] If the initial formation of the reconstituted 95 K band could be measured more accurately, a discrimination between models would be possible: In the one-state and two-states models the 95 K band (*a-s-b*) follows a parabolic time law:

$$a\text{-}s\text{-}b/\overline{AB} = 0.5(k_0k_3 + k_1k_2)t^2 \quad \text{for} \quad t \to 0$$

whereas in the extended one-state model *a-s-b* starts linearly with time:

$$a\text{-}s\text{-}b/\overline{AB} = k_4 t \quad \text{for} \quad t \to 0$$

as can be derived from Tables 1, 3 and 4.

inner membrane surface (Low, 1978) and concomitantly decreases the rate of reaction of *a* with N_2ph-F (Passow et al., 1980*b*). Thus, the combination of this inhibitor with an inward-facing modifier site shifts the equilibrium between the two forms of *a* towards the form that has a low reactivity with respect to N_2ph-F. It is most likely that the states *a* and *a** postulated by the two-state model of H_2DIDS binding are related to the different states of *a* that have been deduced from the work with N_2ph-F.[2]

A further piece of evidence for the capacity of the H_2DIDS binding site to exist in two different states has recently been derived from observations on the effects of dansylation of the red blood cell membrane on anion transport (Legrum, Fasold & Passow, 1980; Lepke & Passow, 1982). Chloride transport across the dansylated membrane is reduced; sulfate transport is enormously enhanced. The effects can be modified when dansylation is carried out in the presence of agents that combine reversibly with the H_2DIDS binding site (e.g., DNDS, DBDS, DAS, APMB). The presence of DBDS or DNDS reduces the rate of dansylation of anion transport controlling modifier sites on band 3 or elsewhere in the bilayer. DAS has no effect while APMB facilitates the inhibition of Cl^- transport and the augmentation of SO_4^{--} transport. These observations have been interpreted on the assumption that the H_2DIDS binding site may exist in two different conformeric states. In one of them dansylation of the anion transport controlling modifier site is easily achieved, in the other this site is inaccessible. The two states have different relative affinities to the noncovalently binding analogues of H_2DIDS listed above. DBDS and DNDS combine preferentially with that conformeric state in which the dansyl chloride binding site is inaccessible. When present at suffciently high concentrations, they transform most of the band 3 protein into that conformer in which the dansyl chloride binding sites show the low reactivity. APMB exerts the opposite behavior. It reacts preferentially with that conformer whose dansyl chloride binding site is easily accessible. At sufficiently high concentrations, it converts the majority of the band 3 molecules into this form and hence facilitates the occurrence of the reciprocal effects on Cl^- and SO_4^{--} transport. DAS assumes an intermediate position. It combines with the two conformers without shifting the distribution ratio between them (Lepke & Passow, 1982).

Finally, Verkman, Dix and Solomon (1981) have studied in temperature jump and stopped-flow experiments the time course of noncovalent binding of DBDS to the H_2DIDS binding site. They find deviations from first-order kinetics that they attribute to conformational transitions that take place after the fast initial binding of the inhibitor. However, in contrast to the models discussed in this paper and other publications from this laboratory, Verkman et al. interpret their results on the assumption, that there exist mutual interactions between the H_2DIDS binding sites on each of the two protomers that constitute the band 3 dimer. Our control experiments (p. 204 and Fig. 5) yielded no direct evidence for such interactions. The equations describing the time course of reversible binding for the two-states model discussed above and the interacting site model of Verkman et al. are formally similar although not identical. Comparative studies under conditions that maximize the differences of the predictions are needed to find out whether or not our present treatment needs to be extended to the inclusion of interactions between adjacent H_2DIDS binding sites. The possibility cannot be excluded that the bulky DBDS molecule shows interactions that do not exist for the less bulky H_2DIDS.

In conclusion of this section, it should be pointed out that the two-states model of the H_2DIDS binding site would fit easily into current concepts of the band 3 mediated anion transport. If one assumes that this site is involved in substrate binding and translocation as previously suggested by Shami et al. (1978), one would expect that the properties of this site change when it moves an anion across the rate limiting barrier and thereby undergoes a change from *cis*-conformation into *trans*-conformation. If the site would be a modifier site, as more recent considerations suggest (Passow, 1982), one could also anticipate that different locations of the transfer site are associated with different conformations at the (essentially immobile) H_2DIDS binding site (Passow et al., 1980*a*, *b*; Passow & Fasold, 1981). Thus the observed deviations of the kinetics of cross-linking from the one-state model are quite likely reflections of different functional states of the transfer site.

[2] The observed inhibition of transport by H_2DIDS that is unilaterally fixed by covalent binding to *b* does not require that the transition $a \rightleftarrows a^*$ be blocked since it has been shown that the modification of *b* alone (Jennings, 1982) and hence possibly the covalent H_2DIDS binding to *b* leads to inhibition. Moreover, the covalent attachment to *b* may even move the H_2DIDS molecule a little further away from the immediate vicinity of *a* such that the interconversion $as\text{-}b \rightleftarrows a^*s\text{-}b$ may take place easier than the interconversion $asb \rightleftarrows a^*sb$, which may occur during the noncovalent binding that precedes covalent bond formation

pH Dependence

The rate of reaction of H_2DIDS with the lysine residues *a* and *b* should vary with pH since thiocyanylation can only take place with the deprotonated form of amino groups. Hence alkalinization should increase the reaction rate since it shifts the equilibrium $R-NH_3^+ \rightleftharpoons R-NH_2+H^+$ to the right. In addition, the pH dependence could also be the result of a conformational change that is induced, e.g., by changes of the charge density at regions of the band 3 molecule or elsewhere in the bilayer that change the organization of the H_2DIDS binding site allosterically.

The sulfonate groups of H_2DIDS contribute to the selectivity of the action on anion transport. They convey to the inhibitor molecule a strong hydrophilic quality that is likely to require binding to a surface that combines hydrophilic and hydrophobic properties and thus could permit the protonation of lys *a* and lys *b*. Significantly enough, in contrast to H_2DIDS, the reaction of certain purely hydrophobic isothiocyanates with buried lysine residues on the band 3 molecule are quite insensitive to variations of pH (Kempf, Sigrist & Zahler, 1979). Thus, it seems useful to try the interpretation of the experimental results on the basis of the two-states model, assuming that the pH dependence is essentially due to variations of the protonation of lys *a* and lys *b* and that superimposed allosteric effects can be neglected.

The hydrogen ion equilibria for the two-states model of the H_2DIDS binding site are quite complex. Each of the two states may be associated with different dissociation constants for each of the two lysine residues *a* and *b*. As may be seen in Fig. 8, altogether there exist 15 different forms that one needs to consider for the description of the pH dependence of the cross-linking reaction. It is evident that the equations for the pH dependence of the various *k*'s are too complex for the calculation of the corresponding pK's. There exists, however, one notable exception. The variations with pH of k_3 are predicted to follow the simple expression $k_3=\bar{k}_3(1+H^+/K_r)$ (*see* p. 204). The data in Fig. 4*b* and *c* show that the experimental observations are in accord with the prediction. Thus one single pH-independent rate constant, $\bar{k}_3$, and one single pK value, pK_r, suffice to describe the pH dependence over the pH range that was accessible to measurements. This suggests that the pK value determined of about 9.9–10.0 pertains indeed to the lysine residue that is directly involved in the thiocyanylation reaction rather than to a superimposed effect on lys *b* of an allosterically linked modifier site.

In addition to k_3, the parameter k_2 should also exhibit a simple pH dependence. According to Fig. 8, $k_2=\bar{k}_2/(1+H^+/K_w)$. However, the scatter of the fitted values k_2(pH) does not permit one to determine $\bar{k}_2$ and K_w with satisfying certainty. The data suggest that pK_w, which pertains to the dissociation of lys *a*, is smaller than or equal to pK_r, which pertains to lys *a*. pK_w seems to be around 7.3 ± 1.8 (95% confidence limits). Independent determinations of the pH dependence of the rate of dinitrophenylation of lys *a* support the contention that pK_w is of about this order of magnitude[3].

The numerical value of a dissociation constant not only depends on the chemical nature of the dissociating group itself but also on the properties of the environment in which the dissociation takes place. Spatial restrictions of the accessibilty to H^+, the dielectric constant, and the electrical charge in the vicinity play an important role. pK_r refers to the pK value that governs the dissociation of lys *b* when a H_2DIDS molecule is covalently attached to lys *a*. This implies that one positive charge in the vicinity (that of lys *a*) had been obliterated by thiocyanylation while two negative charges had been introduced by the two sulfonate groups of the H_2DIDS molecule. Hence the thiocyanylation of lys *b* takes place in the presence of two excess negative charges that are not present in the untreated membrane. These charges should shift the pK to values much higher than 10.5, the value expected for the dissociation of an ε-amino group in an electrically neutral environment (Tanford, 1962). The absence of such a shift may indicate superimposed effects of restricted accessibility, a low dielectric constant and the presence of additional positively charged groups that neutralize the negative charge of the sulfonate groups of H_2DIDS. Such positive charges could possibly exist in the form of the arginine residues that seem to be involved in the control of anion transport (Zaki, 1981, 1982; Wieth, Bjerrum & Borders, 1982).

[3] The only other relationship which is simple enough for experimental examination is the ratio: $k_0/k_1=(\bar{k}_0+\bar{k}_{00}H^+/K_s)/(\bar{k}_1+\bar{k}_{13}H^+/K_v)$. Table 5 shows that the actually observed ratio k_0/k_1 is independent of pH and amounts to about 2.5. The interpretation of this result remains, however, ambiguous. The ratio remains constant under three sets of conditions:

1) $\bar{k}_0/\bar{k}_1=(\bar{k}_{00}/K_s)/(\bar{k}_{13}/K_v)$;

2) $\bar{k}_0 \ll \bar{k}_{00}H^+/K_s$ and $\bar{k}_1 \ll \bar{k}_{13}H^+/K_v$;

3) $\bar{k}_0 \gg \bar{k}_{00}H^+/K_s$ and $\bar{k}_1 \gg \bar{k}_{13}H^+/K_v$.

Conditions 1 and 2 lead to $k_0/k_1=\bar{k}_0/\bar{k}_1$, whereas condition 3 yields $k_0/k_1=(\bar{k}_{00}/K_s)/(\bar{k}_{13}/K_v)$. Our data do not permit one to tell which of the three cases is actually responsible for the observation that the ratio k_0/k_1 is independent of pH.

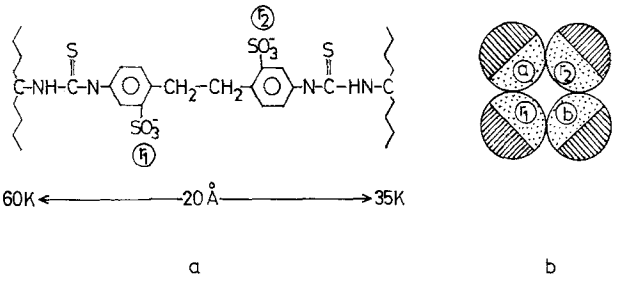

Fig. 9. Distribution of charged groups at the H_2DIDS binding site. Schematic representation of the model considered in the text. (*a*): The H_2DIDS molecule is fixed by thiourea bonds to lys *a* on the 60 K segment and to lys *b* on the 35 K segment of the peptide chain. r_1 and r_2 represent positively charged groups. (*b*): The dashed portions of the four (or possibly five) peptide chains pointing outwards are hydrophobic and in contact with the lipid bilayer. The dotted parts of the peptide chain pointing inwards are hydrophilic and form an aqueous pore

On the basis of the information presented above, one could draw a tentative picture of the distribution of the charged groups at the H_2DIDS binding site. This site would be formed by amino acid residues that belong to different adjacent segments of the peptide chain that traverse the lipid bilayer and that include the lysine residues *a* and *b*. After formation of the cross-link, these residues are about 20 Å apart from one another, i.e., the length of an H_2DIDS molecule. At least two additional charged groups, possibly guanidino groups, could be supplied by neighboring arginine residues that reside on the same or other segments of the peptide chain that also traverse the lipid bilayer. The dissociation of neither lys *a* nor lys *b* produces major effects on Cl^--transport since this transport shows a plateau or a flat maximum that extends over the pH range considered in our experiments (Funder & Wieth, 1976; Brahm, 1977). It may, however, be associated with changes of sulfate transport which decreases in the pH range where the dissociation of lys *b* increases. The differences of pH dependence of the dissociation of lys *b* and of the Cl^--transport support the view (Passow et al., 1980*b*; Passow, 1982) that the H_2DIDS binding site is a modifier site rather than a transfer site. It does not exclude, however, the possibility that the two sites overlap. For example, the positively charged residues r_1 and r_2 in Fig. 9 (perhaps arginine residues) could act as binding sites for the substrate and for the negatively charged sulfonyl groups of the H_2DIDS molecules. This assumption would, however, still require a separate explanation for the small effect of the dissociation of the lysine residues on the capacity of the adjacent arginine residues to engage in Cl^- binding.

The charge configuration depicted in Fig. 9 differs from that in previous publications from this laboratory (Passow & Fasold, 1981; Passow et al., 1980*b*) in so far as we now postulate a minimum of two rather than the previous three additional positively charged groups in the vicinity of lys *a* and lys *b*. This is due to the fact that the previous estimates of pK_r were too low and hence suggested a higher charge density than is necessary for the interpretation of the present results. Our previous work was done entirely with intact red cells. At that time we were not yet aware of the problems associated with the use of intact cells (*see* p. 210) that restrict the experiments to a narrow pH range.

We thank Drs. D. Schubert, P. Wood, and E. Grell for their comments on the manuscript and Mr. E. Golombeck for streamlining the equations describing the two-states model. The work was supported in part by the Deutsche Forschungsgemeinschaft.

References

Barzilay, M., Ship, S., Cabantchik, Z.I. 1979. Anion transport in red blood cells. Chemical properties of anion recognition sites as revealed by structure-activity relationships of aromatic sulfonic acids. *Membrane Biochem.* **2**:227–254

Brahm, J. 1977. Temperature-dependent changes of chloride transport kinetics in human red cells. *J. Gen. Physiol.* **70**:283–306

Brown, K.M., Dennis, J.E. 1972. Derivative free analogues of the Levenberg-Marquardt and Gauss algorithms for the nonlinear least squares approximation. *Numer. Math.* **18**:289–297

Cabantchik, Z.I., Rothstein, A. 1974. Membrane proteins related to anion permeability of human red blood cells. I. Localization of disulfonic stilbene binding sites in proteins involved in permeation. *J. Membrane Biol.* **15**:207–226

Cousin, J., Motais, R. 1978. A structure activity study of some drugs acting as reversible inhibitors of chloride permeability in red cell membranes: Influence of ring substituents. *In:* Cell Membrane Receptors for Drugs and Hormones: A Multidisciplinary Approach. R.W. Straub and L. Bolis, editors. pp. 219–225. Raven Press, New York

Dorst, H.J., Schubert, D. 1979. Self-association of band 3-protein from human erythrocyte membranes in aqueous solutions. *Hoppe-Seyler's Z. Physiol. Chem.* **360**:1605–1618

Fletcher, R., Powell, M.J.D. 1963. A rapid descent method for minimization. *Comput. J.* **6**:163–168

Fröhlich, O. 1982. The external anion binding site of the human erythrocyte anion transporter: DNDS binding and competition with chloride. *J. Membrane Biol.* **65**:111–123

Funder, J., Wieth, J.O. 1976. Chloride transport in human erythrocytes and ghosts: A quantitative comparison. *J. Physiol. (London)* **262**:679–698

Halestrap, A.P. 1976. Transport of pyruvate and lactate into human erythrocytes. *Biochem. J.* **156**:193–207

IMSL routine ZXSSQ. 1980. IMSL Library (8th ed). International Mathematical and Statistical Library, Inc., Houston

Jennings, M.L. 1982. Reductive methylation of two H_2DIDS-binding lysine residues on band 3, the human erythrocyte anion transport protein. *Biophys. J.* **37**:177*a*

Jennings, M.L., Passow, H. 1979. Anion transport across the erythrocyte membrane, *in situ* proteolysis of band 3 protein, and cross-linking of proteolytic fragments by 4,4′-diisothiocyano dihydrostilbene-2,2′-disulfonate. *Biochim. Biophys. Acta* **554**:498–519

Kampmann, L., Lepke, S., Fasold, H., Passow, H. 1982. The kinetics of intramolecular crosslinking of the band 3 protein by 4,4′-diisothiocyanato dihydrostilbene-2,2′-disulfonic acid (H_2DIDS). *In:* Protides of the Biological Fluids, Proceedings of the 29th Colloquium. H. Peeters, editor. pp. 275–278. Pergamon, Oxford

Kaplan, J., Scorah, K., Fasold, H., Passow, H. 1976. Sidedness of the inhibitory action of disulfonic acids on chloride equilibrium exchange and net transport across the human erythrocyte membrane. *FEBS Lett.* **62**:182–185

Kempf, C., Sigrist, H., Zahler, P. 1979. Covalent modification of human erythrocyte band 3 and phosphate transport inhibition by acryl isothiocyanates. *Experientia* **35**:937

Knauf, P.A., Rothstein, A. 1971. Chemical modification of membranes. I. Effects of sulfhydryl and amino-reactive reagents on anion and cation permeability of the human red blood cell. *J. Gen. Physiol.* **58**:190–210

Knauf, P.A., Law, F.Y. 1980. Relationship of net anion flow to the anions exchange system. *In:* Membrane Transport in Erythrocytes. U.V. Lassen, J.O. Wieth, and H.H. Ussing, editors. pp. 488–493. Alfred Benzon Symposium 14, Munksgaard, Copenhagen

Legrum, B., Fasold, H., Passow, H. 1980. Enhancement of anion equilibrium exchange by dansylation of the red blood cell membrane. *Hoppe-Seyler's Z. Physiol. Chem.* **361**:1573–1590

Lepke, S., Fasold, H., Pring, M., Passow, H. 1976. A study of the relationship between inhibition of anion exchange and binding to the red blood cell membrane of 4,4′-diisothiocyano stilbene-2,2′-disulfonic acid (DIDS) and its dihydro derivate (H_2DIDS). *J. Membrane Biol.* **29**:147–177

Lepke, S., Passow, H. 1982. Inverse effects of dansylation of the red cell membrane on the band 3-protein-mediated transport of sulfate and chloride. *J. Physiol. (London)* **328**:27–48

Low, P.S. 1978. Specific cation modulation of anion transport across the human erythrocyte membrane. *Biochim. Biophys. Acta* **514**:264–273

Maddy, A.H. 1964. A fluorescent label for the outer components of the plasma membrane. *Biochim. Biophys. Acta* **88**:390–399

Nigg, E.A., Bron, C., Giradet, M., Cherry, R.J. 1980. Protein associations in erythrocyte membranes demonstrated by protein diffusion measurements. *Experientia* **36**:729

Pappert, G., Schubert, D. 1981. Self-association of band 3 protein from erythrocyte membranes in solutions of a non-ionic detergent, ammonyx-LO. *In:* Protides Biological Fluids, Proceedings of the 29th Colloquium. H. Peeters, editor. pp. 117–120. Pergamon, Oxford

Passow, H. 1982. Anion transport-related conformational changes of the band 3 protein in the red cell membrane. *In:* Membranes and Transport. Vol. II, pp. 451–460. A.N. Martonosi, editor. Plenum, New York

Passow, H., Fasold, H. 1981. On the mechanism of band-3-protein-mediated anion transport across the red blood cell membrane. *In:* Advances of Physiological Sciences. Vol. 6. Genetics, Structure and Function of Blood Cells. S.R. Hollán, G. Gárdoz, and B. Sarkadi, editors. pp. 249–261. 28th Int. Congress of Physiol. Sci. Académiai Kiado, Budapest

Passow, H., Fasold, H., Gärtner, E.M., Legrum, B., Ruffing, W., Zaki, L. 1980*b*. Anion transport across the red blood cell membrane and the conformation of the protein in band 3. *Ann. N. Y. Acad. Sci.* **341**:361–383

Passow, H., Fasold, H., Jennings, M.L., Lepke, S. 1982. The study of the anion transport protein (band 3 protein) in the red cell membrane by means of tritiated 4,4′-diisithiocyano-dihydro-stilbene-2,2′-disulfonic acid (H_2DIDS). *In:* Chloride Transport in Biological Membranes. A. Zadunaisky, editor. pp. 1–31. Academic Press, New York

Passow, H., Fasold, H., Zaki, L., Schuhmann, B., Lepke, S. 1975. Membrane proteins and anion exchange in human erythrocytes. *In:* Proceedings of the 9th FEBS Meeting, Budapest 1974. Vol. 35. I. Biomembranes: Structure and Function. G. Gárdos, and I. Szász, editors. pp. 197–214. Akadémiai Kiado, Budapest

Passow, H., Kampmann, L., Fasold, H., Jennings, M.L., Lepke, S. 1980*a*. Mediation of anion transport across the red blood cell membrane by means of conformational changes of the band 3 protein. *In:* Membrane Transport in Erythrocytes. Alfred Benzon Syposium 14. U.V. Lassen, H.H. Ussing, and J.O. Wieth, editors. pp. 345–372. Munksgaard, Copenhagen

Peterson, G.L. 1979. Review of the Folin phenol quantitation method of Lowry, Rosebrough, Farr and Randall. *Anal. Biochem.* **100**:201–220

Shami, Y., Rothstein, A., Knauf, P.A., McCulloch, L. 1978. Identification of the Cl^- transport site of human red blood cells by a kinetic analysis of the inhibitory effects of a chemical probe. *Biochim. Biophys. Acta* **508**:357–363

Ship, S., Shami, Y., Breuer, W., Rothstein, A. 1977. Synthesis of tritiated 4,4′-diisothiocyano-2,2′-stilbene disulfonic acid ([^{3}H]DIDS) and its covalent reaction with sites related to anion transport in human red blood cells. *J. Membrane Biol.* **33**:311–323

Steck, T.L. 1978. The band 3 protein of the human red cell membrane: A review. *J. Supramol. Struct.* **8**:311–324

Tanford, C. 1962. The interpretation of hydrogen ion titration curves of proteins. Advances in Protein Chemistry, Vol. 17, pp. 69–165. C.B. Anfinsen and J.T. Edsall, editors. Academic Press, New York

Verkman, A.S., Dix, J.A., Solomon, A.K. 1981. Anion transport inhibitor binding to band 3 in red blood cell membranes. *J. Gen. Physiol.* (*in press*)

Weinstein, R.S., Khodadad, J.K., Steck, T.L. 1980. Band 3 protein is a tetramer in the human red cell membrane. *J. Cell Biol.* **87**:209*a*

Wieth, J.O., Bjerrum, P.J., Borders, C.L. 1982. Irreversible inactivation of red cell chloride exchange with phenylglyoxal – an arginine-specific reagent. *J. Gen. Physiol.* **79**:283–312

Wood, P.D., Passow, H. 1981. Techniques for the modification of the intracellular composition of the red blood cells. *In:* Techniques in the Life Sciences. Physiology, Vol. P1/I, pp. 1–43. P.F. Baker, editor. Elsevier, County Clare (Ireland)

Zaki, L. 1981. Inhibition of anion transport across red blood cells with 1,2-cyclohexanedione. *Biochem. Biophys. Res. Commun.* **99**:243–251

Zaki, L. 1982. The effect of arginine specific reagents on anion transport across red blood cells. *In:* Protides Biological Fluids. Proceedings of the 29th Colloquium. H. Peeters, editor. pp. 270–282. Pergamon, Oxford

Zaki, L., Fasold, H., Schuhmann, B., Passow, H. 1975. Chemical modification of membrane proteins in relation to inhibition of anion exchange in human red blood cells. *J. Physiol. (London)* **86**:471–494

Received 5 January 1982; revised 19 May 1982